

A Raman spectroscopic study of glasses in the system CaO–MgO–SiO₂

PAUL McMILLAN

Department of Chemistry
Arizona State University, Tempe, Arizona 85287

Abstract

The Raman spectra of a number of glasses in the system CaO–MgO–SiO₂ have been prepared using solar furnace techniques. The spectra of glasses along the SiO₂–CaO, SiO₂–MgO and SiO₂–Ca_{0.5}Mg_{0.5}O joins are similar to those obtained in other studies, and are interpreted in terms of vibrations of tetrahedral silicate units with zero, one, two, three and four non-bridging oxygens, consistent with previous discussions. Some glasses were prepared with bulk compositions within the CaO–MgO–SiO₂ two-liquid field, using both a “normal” and a fast quench rate. The normal-quenched glasses were opaque and unmixed, the fast-quenched samples transparent and homogeneous. Both sets of samples had identical spectra, and the implications of this are discussed. Finally, a number of samples with varying Ca/Mg ratio at constant high silica content were studied. Their Raman spectra are discussed along with results of previous studies on alkali and alkaline earth silicate glass systems to develop a molecular site model which describes the effect of changing metal cation on the distribution of silicate species.

Introduction

A considerable number of studies have used Raman spectroscopy to investigate the structures of silicate glasses and melts, many of which have been applied to understanding properties important in geological processes. In the present study, a number of glasses were prepared in the system CaO–MgO–SiO₂ using solar furnace melting and fast quench techniques. There have been several previous studies on glasses and melts in this system (e.g., Etchepare, 1970a, 1972; Konijendijk, 1975; Brawer and White, 1977; Sharma et al., 1979; Sharma and Yoder, 1979; Virgo et al., 1980; Kashio et al., 1980; Mysen et al., 1980a,b, 1982a,b; Mysen and Virgo, 1980; Tsunawaki et al., 1981; McMillan et al., 1981; McMillan and Piriou, 1983; Piriou and McMillan, 1983a,b) whose results are compared with the present observations. Finally, a number of samples with bulk compositions within the two-liquid field of the liquidus CaO–MgO–SiO₂ phase diagram were prepared by quenching from the liquid at different quench rates. The Raman spectra of these glasses give some insight into the nature of unmixing in this system, and lead to a discussion of the rôle of metal cations in determining the structures of these and other silicate glasses and melts.

Experimental procedure

Sample preparation and characterization

Glass samples for this study were prepared from reagent-grade oxide mixes or gels by solar melting at the French solar furnace facility (CNRS Odeillo). Temperatures at the sample could not

be controlled or accurately measured, but were estimated at 2000–2500°C. Normal quenching (NQ) was achieved by simply removing the sample from the beam and allowing to cool in air, to give a quench rate of around 10³°C/s. Super-quenched (SQ) samples were obtained by splat quenching on the water-cooled sample stage. The quench rate by this method is of the order of 10⁵–10⁶°C/s. Melting was ascertained by visual observation of the samples during heating, and by optical, Raman and X-ray study of the quenched products. Further details of this preparation method are discussed in Coutures et al., (1978), McMillan (1981), and McMillan et al. (1982).

Samples were analyzed using a Cameca MS-46 electron microprobe with a 15 kV accelerating voltage and near 25 nA beam current for a 2 μm spot size. Data were reduced using the program FRAME (Heinrich, 1972). Twenty to thirty point counts were obtained for each sample, and a relative homogeneity index H was calculated following similar reasoning to Boyd and Finger (1975) (see McMillan et al., 1982). Values of H near unity indicate that the sample is homogeneous in that oxide component. Most glass samples in this study were found to be homogeneous, and Raman spectra obtained from different parts of a given sample were identical. Some samples with compositions within the CaO–MgO–SiO₂ miscibility gap (Levin et al., 1964, p. 211; Fig. 1) were found to be inhomogeneous, and were analyzed by X-ray fluorescence using a Philips PW 1410 vacuum spectrometer and the low-dilution disc method of Thomas and Haukka (1978). Some such samples showed differences in Raman spectra between parts of the same sample, as discussed in the text. Analytical results are reported in Table 1, and sample compositions studied are shown in Figure 1.

Raman spectroscopy

All transparent NQ samples were polished for polarized 90° Raman scattering, while opaque glasses were run by glancing

Table 1. Glass compositions studied in the CaO-MgO-SiO₂ system.

(a) The SiO ₂ -CaMgSiO ₄ join (Figures 3, 4).									
Sample	mole % oxide			method ^(a)		homogeneity ^(b)			
	CaO	MgO	SiO ₂	ϵ ^(c)	# ^(d)	CaO	MgO	SiO ₂	
1 SQ ^(e)	33.2	32.4	34.3	100.0	XRF	-	-	-	-
2 SQ	34.5	31.8	33.7	100.0	SEM	-	-	-	-
2 SQ	35.9	27.8	36.2	101.4	EMP	27	1	1	1
2 SQ	0.6 ^(f)	0.7	0.6	1.8	-	-	-	-	-
2 SQ	37.4	27.4	35.2 ^(g)	100.0	AA	-	-	-	-
3 NQ	33.5	25.4	41.1	99.4	EMP	21	1	1	1
3 NQ	0.9	0.7	0.9	0.9	-	-	-	-	-
3 NQ	34.6	24.7	40.8	100.0	AA	-	-	-	-
4 NQ	32.0	23.3	44.7	100.0	EMP	18	1	1	1
4 NQ	0.7	0.7	0.7	2.4	-	-	-	-	-
4 NQ	33.1	24.2	42.7	100.0	AA	-	-	-	-
5 NQ	31.3	22.7	45.9	99.5	EMP	21	1	1	1
5 NQ	0.8	0.8	0.8	1.3	-	-	-	-	-
5 NQ	30.7	23.2	46.2	100.0	AA	-	-	-	-
6 NQ	29.5	22.4	48.1	100.8	EMP	17	1	1	1
6 NQ	0.5	0.7	0.7	1.1	-	-	-	-	-
6 NQ	31.1	22.4	46.5	100.0	AA	-	-	-	-
7 NQ	27.9	21.2	51.0	101.1	EMP	24	2	2	2
7 NQ	1.4	1.1	1.5	3.8	-	-	-	-	-
7 NQ	28.8	21.3	49.9	100.0	AA	-	-	-	-
8 NQ	27.8	20.2	52.0	98.9	EMP	20	1	1	1
8 NQ	0.4	0.5	0.4	1.3	-	-	-	-	-
8 NQ	28.2	20.4	51.4	100.0	AA	-	-	-	-
9 NQ	26.0	18.0	56.0	99.6	EMP	21	1	2	2
9 NQ	0.8	1.3	1.8	2.0	-	-	-	-	-
9 NQ	25.3	19.3	55.4	100.0	AA	-	-	-	-
10 SQ	21.8	20.5	57.6	99.4	EMP	21	1	1	1
10 SQ	0.6	0.4	0.5	1.8	-	-	-	-	-
10 NQ	22.1	21.8	56.1	100.0	AA	-	-	-	-
SiO ₂	-	-	100.0	100.0	(h)	-	-	-	-
NQ	-	-	-	-	-	-	-	-	-

angle reflection. The SQ glasses were generally too small and friable for mounting and polishing, and unpolarized or partially-polarized spectra were obtained from unpolished samples. Most spectra were obtained at CNRS Bellevue (France) using a Spectra-Physics 165 Ar⁺ laser and Coderg PHO double monochromator. A number of spectra for samples of poor optical quality were run at ENSTA, Palaiseau with a Coherent Ar⁺ laser and Coderg T800 triplet monochromator. Glass spectra were obtained using the 4800 or 5145 Å lines of the argon lasers, with 500–1000 mW power at the sample, and resolving slits of near 4 cm⁻¹. The room-temperature spectra reported here were not reduced to remove effects of thermal population (e.g., Leadbetter and Stringfellow, 1974; Piriou and Alain, 1979). This procedure removes the pseudo-band near 50–100 cm⁻¹ and reduces the relative intensity below around 600 cm⁻¹ (Hass, 1969; Shuker and Gammon, 1970), but does not substantially change the band contours discussed here.

Unresolved bands were decomposed using a curve-fitting technique with a DuPont 310 curve-resolver as described previously (McMillan et al., 1982). Results of curve-fitting experiments for glasses along the SiO₂-CaMgSiO₄ join are shown in Figure 4 and Table 2, and are discussed below. The method followed is illustrated in Figure 2 for sample 9 with 52 mole % SiO₂. The component bands fitted at 1058, 972 and 868 cm⁻¹ correspond to the obvious features in the experimental spectrum indicated by arrows. The intensities of these bands were optimized to reproduce the high- and low-frequency sides of the observed band contour, while the 914 and 1154 cm⁻¹ components were introduced to complete the fit. In the present

Table 1. (cont.)

Sample	mole % oxide			method		homogeneity			
	CaO	MgO	SiO ₂	ϵ	#	CaO	MgO	SiO ₂	
(b) The CaMgSiO ₄ -SiO ₂ miscibility gap (Figure 7).									
SiO ₂ SQ	-	-	99.8	98.7	EMP	22	-	-	1
11 NQ	20.7	14.6	64.6	0.7	1.7	96.2 ^(j)	EMP	22	2
4	1.5	1.6	2.9	1.0	-	-	-	-	-
11 NQ	20.8	15.2	64.0	104.0 ^(k)	XRF	-	-	-	-
12(1) NQ	22.3	14.4	63.3	95.3	EMP	12	5	5	6
(m)	3.4	2.4	4.5	8.2	-	-	-	-	-
12(2) NQ	4.7	2.0	92.5	93.8	EMP	11	17	29	10
12 NQ	5.5	5.5	9.3	8.9	-	-	-	-	-
12 NQ	14.5	11.3	74.2	107.5	XRF	-	-	-	-
13 NQ	7.0	4.4	88.5	93.4	EMP	23	13	11	9
13 NQ	4.9	3.2	8.1	2.1	-	-	-	-	-
13 NQ	8.9	7.5	83.5	108.2	XRF	-	-	-	-
11 SQ	17.9	13.8	68.2	99.6	EMP	27	2	3	4
12 SQ	1.5	1.6	2.9	1.7	-	-	-	-	-
12 SQ	15.9	12.1	71.9	100.4	EMP	26	6	6	7
13 SQ	3.2	2.9	6.0	1.0	-	-	-	-	-
13 SQ	7.6	6.1	86.3	99.8	EMP	22	2	2	2
	0.8	0.7	1.2	1.2	-	-	-	-	-
(c) The SiO ₂ -CaO join (Figure 8)									
14 SQ	59.2	-	40.8	100.7	EMP	24	1	-	1
15 SQ	0.8	-	0.8	1.4	-	-	-	-	-
15 SQ	49.1	-	50.9	100.9	EMP	21	1	-	1
16 NQ	0.5	-	0.5	1.0	-	-	-	-	-
16 NQ	42.2	-	57.8	100.5	EMP	21	1	-	1
17 NQ	0.7	-	0.7	1.3	-	-	-	-	-
17 NQ	37.8	-	62.2	98.7	EMP	17	2	-	2
18 NQ	0.7	-	0.7	1.4	-	-	-	-	-
18 NQ	34.6	-	65.3	99.9	EMP	19	2	-	2
19 NQ	1.8	-	1.8	1.1	-	-	-	-	-
19 NQ	28.2	-	71.8	98.4	EMP	18	4	-	4
20 NQ	3.5	-	3.5	1.8	-	-	-	-	-
20 NQ	15.2	-	84.8	97.0	EMP	23	14	-	8
20 NQ	7.7	-	7.7	3.9	-	-	-	-	-
20 NQ	11.2	-	88.8	102.6	XRF	-	-	-	-

Table 1. (cont.)

Sample	mole % oxide			method		homogeneity			
	CaO	MgO	SiO ₂	ϵ	#	CaO	MgO	SiO ₂	
(d) The SiO ₂ -MgO join (Figure 8)									
21 SQ	-	53.0	47.0	100.0	EMP	29	-	1	2
22 SQ	-	1.2	1.2	126	-	-	-	-	-
22 SQ	-	51.0	49.0	101.1	EMP	19	-	1	2
23 SQ	-	1.5	1.5	1.8	-	-	-	-	-
23 SQ	-	29.8	70.1	100.0	EMP	23	-	1	1
23 NQ	-	0.6	0.6	1.5	-	-	-	-	-
23 NQ	-	30.3	69.6	93.6	EMP	19	-	5	4
23 NQ	-	2.7	2.7	1.0	-	-	-	-	-
23 NQ	-	30.9	69.1	99.6	XRF	-	-	-	-
(e) High-silica samples (Figure 9).									
19 NQ	28.2	-	71.8	98.4	EMP	18	4	-	4
11 SQ	3.5	-	3.5	1.8	-	-	-	-	-
11 SQ	17.9	13.8	68.2	99.6	EMP	27	2	3	4
12 SQ	1.5	1.6	2.9	1.7	-	-	-	-	-
12 SQ	15.9	12.1	71.9	100.4	EMP	26	6	6	7
23 SQ	3.2	2.9	6.0	1.0	-	-	-	-	-
23 SQ	-	29.8	70.1	100.0	EMP	23	-	1	1
	-	0.6	0.6	1.5	-	-	-	-	-

- Notes: (a) Analysis method: XRF - X-ray fluorescence, EMP-electron microprobe, AA - atomic absorption analysis in the Université de Paris VI, SEM-energy-dispersive scanning electron microscopy. (b) Homogeneity index (see section on Experimental Techniques). (c) Sum of weight per cent oxides for EMP and XRF. (d) Number of points in EMP traverse. (e) SQ -super quench; NQ - normal quench (see text). (f) Two standard deviations (2 σ) for EMP analyses. (g) SiO₂ by difference. (h) High-purity silica samples from Electro-Quartz Co., France. (Tetrasil SE: < 10 ppm H₂O, < 1 ppm impurities). (j) Poor EMP totals due to differential polish on surface of unmixed samples. (k) Poor XRF totals due to standard curve used (Problems in making discs with high CaO, MgO contents). (m) Sample 12-NQ analyzed as two composition populations (1) and (2).

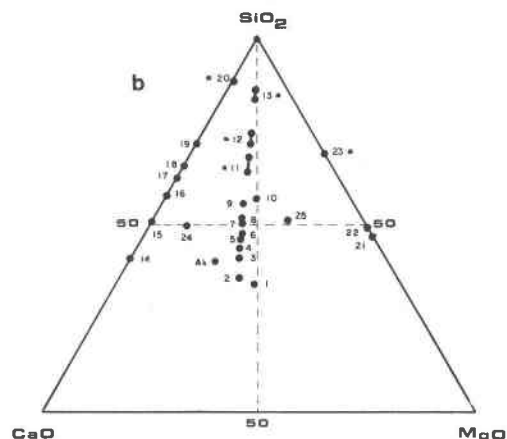
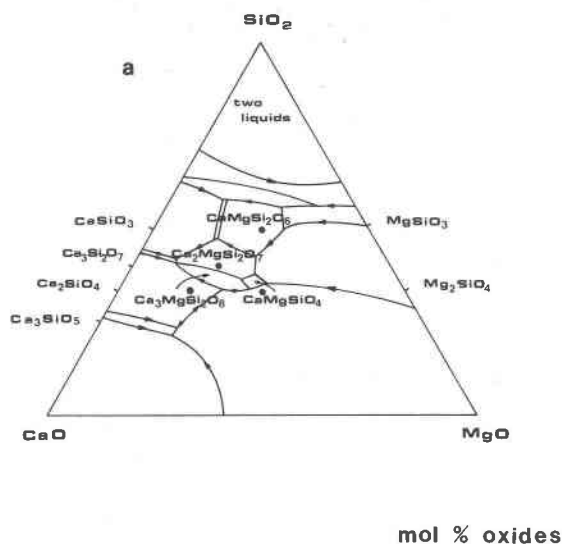


Fig. 1. (a) Schematic liquidus phase diagram for the system CaO-MgO-SiO₂, redrawn from Levin et al. (1964). (b) Compositions of glasses examined in this study. Numbers correspond to sample numbers in Table 1. Those marked with an asterisk (11, 12, 13, 20, 23) are average bulk compositions of inhomogeneous samples. The two points shown connected by a tie-line for samples 11, 12 and 13 refer to NQ (higher silica) and SQ (lower silica) samples (see Table 1).

study, it was assumed that these Gaussian components did not change in position or width with silica content, in order to provide some constraints for the fitting procedure. Although the fitting method is obviously rather crude, and the above assumption not obviously valid, the major fitted bands agree generally with those found by other workers for similar systems (Mysen et al., 1980a,b,c,d, 1981a,b, 1982a,b; Mysen and Virgo, 1980a). The validity of such fits has been discussed by Mysen et al. (1982b), McMillan and Piriou (1983), and McMillan (1984). The polarization characteristics of the component bands were measured from their intensities in the parallel (VV) and perpendicular (VH) polarized spectra. The depolarization ratios, $\rho = (I_{VH}/I_{VV})$, are quoted in Table 2. Only totally symmetric

vibrations of a cubic point group are completely polarized, with $\rho = 0$. Asymmetric modes of all point groups are depolarized, with $\rho = 3/4$ for plane-polarized incident light, while other symmetric vibrations are polarized with $0 < \rho < 3/4$ (Herzberg, 1945, p. 246-249). In the present discussion, the degree of polarization is used to compare polarized bands with different values of ρ between 0 and 0.75.

Results and discussion

The SiO₂-CaMgSiO₄ glass series

The polarized Raman spectra of these glasses are shown in Figure 3. Due to selective evaporation of component oxides during the solar furnace preparations, samples 2 to 9 lie slightly off the join, but this is not believed to have a major effect on the spectral variations with silica content. The spectra obtained are comparable with the results of previous studies on the SiO₂-CaMgSiO₄ system (e.g., Virgo et al., 1980; Mysen et al., 1980a, 1982a). Sample 10 was prepared in a conventional Deltech furnace, and has a composition on the low-silica limit of the liquidus SiO₂-CaMgSiO₄ miscibility gap. Those samples with compositions within the two-liquid field are discussed in a later section. Samples 1 and 2 could only be obtained using the super-quench technique, and no polarization information was obtained for sample 2, while the spectrum of sample 1 is only partially polarized (McMillan et al., 1981). The spectra are most easily discussed in three sections: the high-frequency region above 800 cm⁻¹; a low-frequency region between 400 and 700 cm⁻¹; and the mid-range region from 700 to 800 cm⁻¹.

The high-frequency region. Sample 1 at the orthosili-

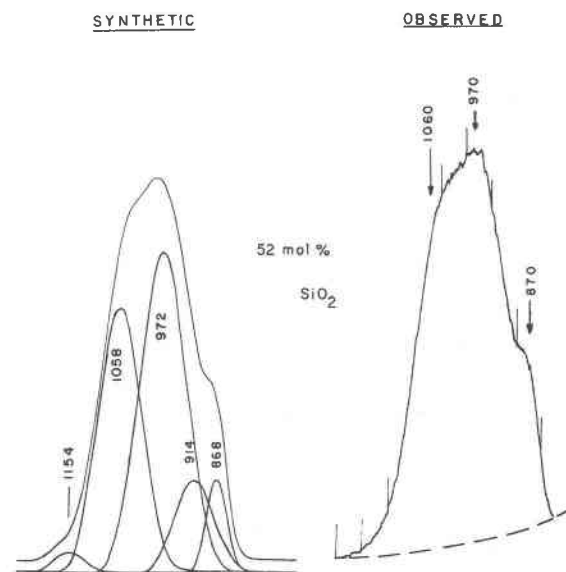


Fig. 2. Results of a curve-fitting experiment on the high-frequency region of sample number 9 (52 mol % silica) along the SiO₂-CaMgSiO₄ glass join.

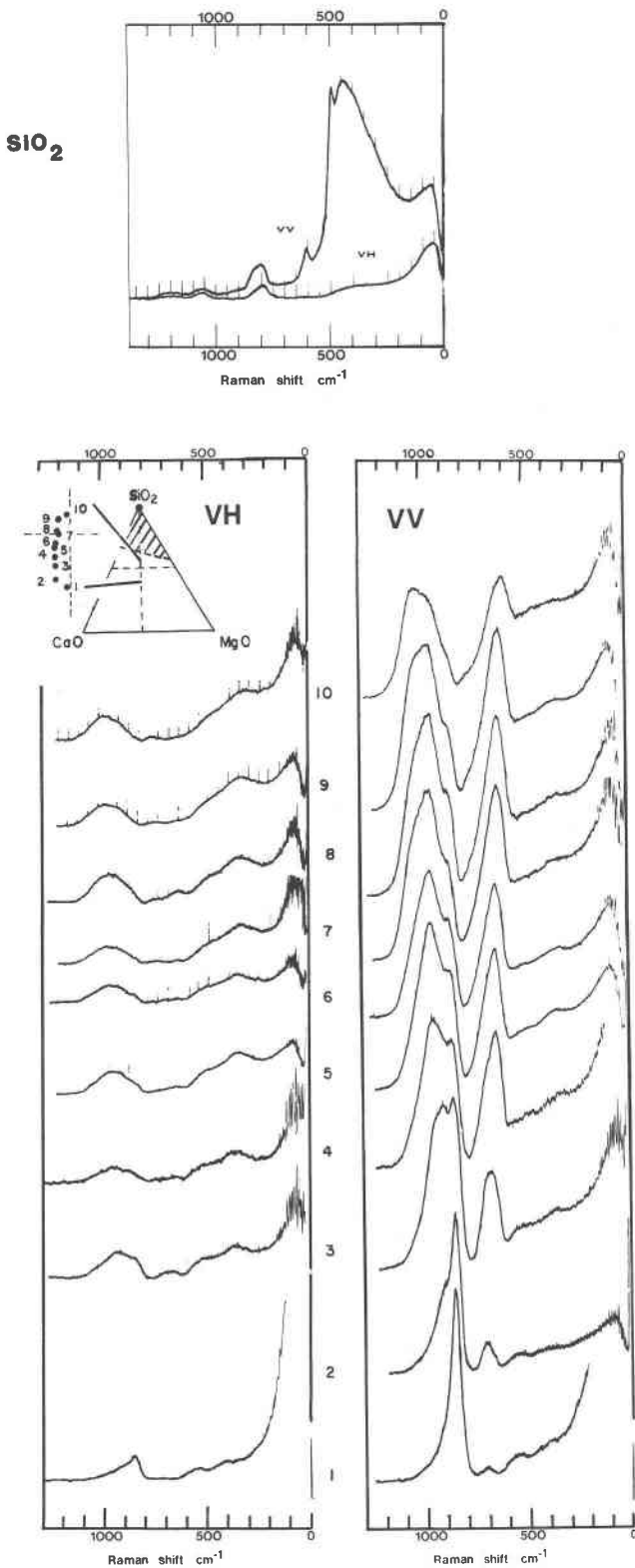


Fig. 3. Polarized (VV and VH) Raman spectra of glasses 1–10 near the $\text{SiO}_2\text{-CaMgSiO}_4$ join.

cate composition shows a strong band near 850 cm^{-1} with an asymmetric tail to higher frequency. The 850 cm^{-1} band may be completely polarized within experimental uncertainty (McMillan et al., 1981; Piriou and McMillan, 1983a), while the high-frequency component has a high depolarization ratio. With increasing silica content, the 850 cm^{-1} band decreases in relative intensity, while new bands grow at higher frequency. At sample 3, the major high frequency peak is at 910 cm^{-1} , with a pronounced shoulder near 1000 cm^{-1} . Between samples 4 and 9, this shoulder develops into the major band in the spectrum, while a further shoulder near 1050 cm^{-1} becomes apparent for sample 7. This 1050 cm^{-1} shoulder increases in relative intensity between samples 7 and 10, to become the dominant high-frequency band of sample 10. The VH spectra show all these bands to be highly, but not completely polarized. The VH polarized spectra also show different asymmetric band contours to the corresponding VV spectra, suggesting that the various components bands have different depolarization ratios. The spectrum of vitreous silica at the top of Figure 3 shows two weak bands near 1200 and 1060 cm^{-1} which Furukawa et al. (1981) found to be depolarized ($\rho \sim 0.75$). Seifert et al. (1982) and Mysen et al. (1982a) have suggested that the broad 1200 cm^{-1} band may have two components, at 1209 and 1160 cm^{-1} .

For a clearer view of spectral changes as a function of silica content, these high-frequency bands were deconvoluted into Gaussian components, as described above. The results of this curve-fitting are shown in Figure 4 and Table 2. Four major component bands were found for samples 1–10; at 862 , 906 , 972 and 1056 cm^{-1} , in reasonable agreement with Mysen et al., (1980a, 1982a,b) and Mysen and Virgo (1980). These were all highly polarized, with ρ ranging from < 0.1 (for the 862 cm^{-1} band) to around 0.2 . The variation in relative intensity of these major bands with silica content is shown in Figure 5. The 862 cm^{-1} band is dominant at the orthosilicate composition, the 906 cm^{-1} band near the pyrosilicate with 40 mole % silica, and the 972 cm^{-1} band at the metasilicate composition (50 mole % silica). The 1056 cm^{-1} band has not yet reached a maximum in relative intensity at 58 mole % silica. These variations are similar to those observed by Furukawa et al. (1981) for the 950 cm^{-1} and 1100 cm^{-1} bands in the $\text{SiO}_2\text{-Na}_2\text{O}$ glass series, and who found the 1100 cm^{-1} band to be maximized at the disilicate composition with 67 mole % silica. On the basis of the positions, intensities and polarization characteristics of these bands, the silica content at which they have maximum intensity, and comparison of corresponding glass and crystal spectra, previous workers have concluded that the 862 , 906 , 972 and 1056 cm^{-1} bands correspond to symmetric silicon–oxygen stretching vibrations of silicate tetrahedral units with respectively four, three, two and one non-bridging oxygen (e.g., Brawer and White, 1975; Verweij and Konijnendijk, 1976; Virgo et al., 1980; Mysen et al., 1980a, 1982a; Furukawa et al., 1981 and

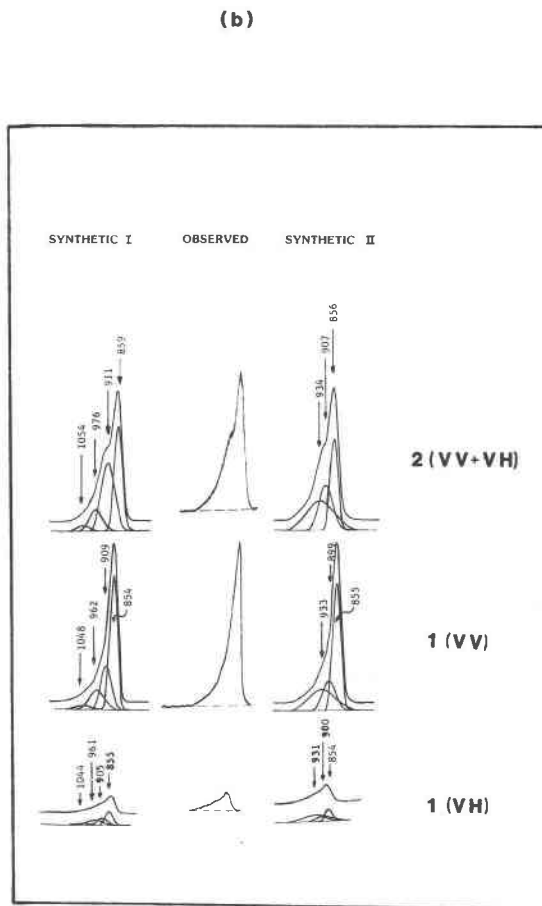
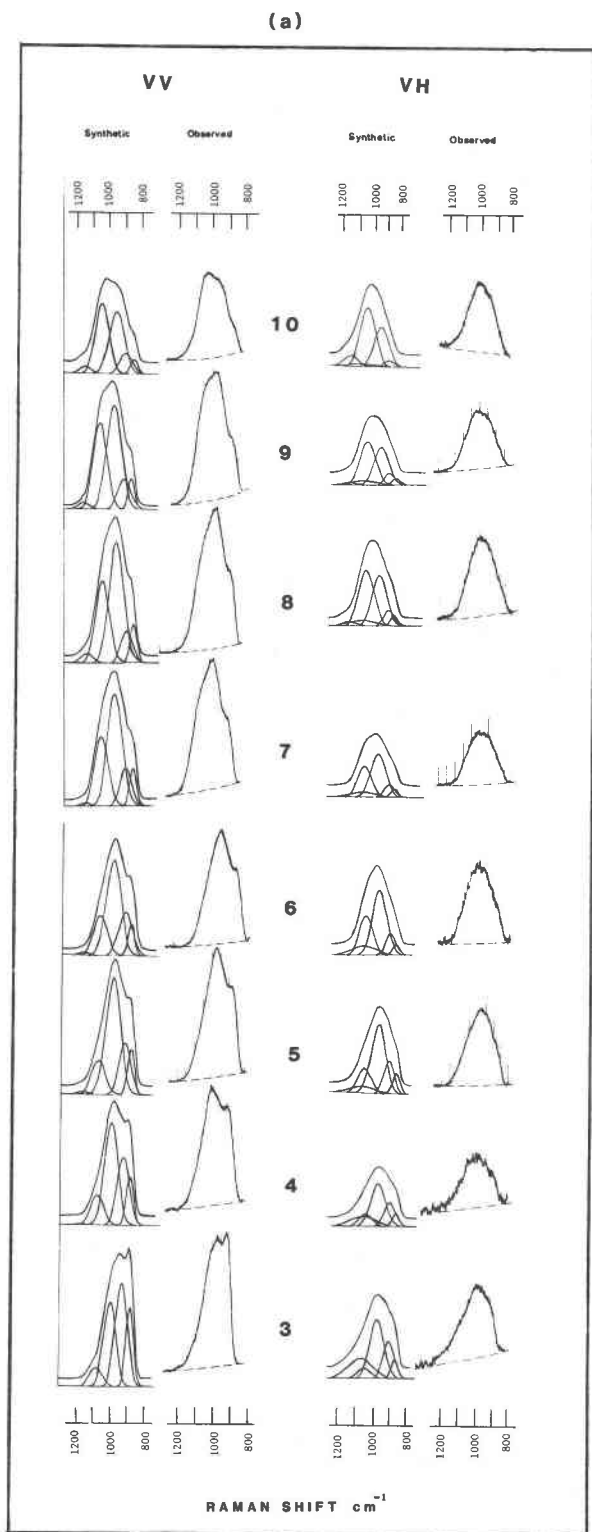


Fig. 4. Curve-fitting experiments on the high-frequency bands of the $\text{SiO}_2\text{-CaMgSiO}_4$ glass series in Fig. 3. In each case, the observed unresolved band contour is shown at right for comparison with the synthetic sum of components. The dashed line shows the assumed baseline, which could not be reproduced for the synthetic reconstruction. Measured component band positions are given in Table 2, along with relative band intensities, half-widths and depolarization ratios, and a general discussion of these data.

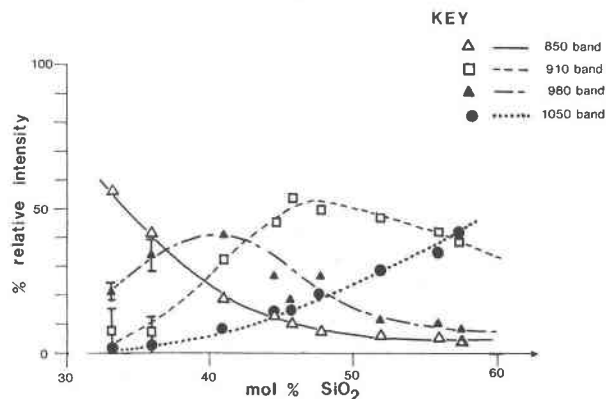


Fig. 5. Relative high-frequency component band intensities from VV polarized spectra in the SiO₂-CaMgSiO₄ glass series (from Fig. 4 and Table 2). The error bars shown for the component bands for samples 1 and 2 represent the relative intensities obtained from alternative deconvolutions I and II, which are thought to be extreme cases (see Table 2 and Fig. 4).

many others: summarized in McMillan, 1984). These units are shown schematically in Figure 6, and are referred to here as SiO₄, -SiO₃, =SiO₂, and ≡SiO groups. These are equivalent to the Q⁰, Q¹, Q², and Q³ species referred to by other workers (e.g., Matson et al., 1983) in notation borrowed from NMR spectroscopic studies (Englehardt et al., 1975). The present notation is used here for its pictorial value, and its simple extension to aluminosilicate systems (McMillan et al., 1982). There are a number of other weak components present in the high-frequency spectra associated with the above major bands, which may be due to asymmetric stretching vibrations of these units within the glass (see e.g., Furukawa and White, 1980; Mysen et al., 1980a; Furukawa et al., 1981; Matson et al., 1983; McMillan, 1984; also footnote to Table 2).

There have been a number of interpretations of the 1200 and 1060 cm⁻¹ bands observed for vitreous silica (see McMillan, 1984). For the purposes of the present discussion, these are assigned to asymmetric silicon-oxygen stretching motions within the fully-polymerized silica glass framework (McMillan et al., 1982). In the present notation, this framework is represented as =Si=.

The low-frequency region. The spectrum of sample 1 shows a weak, polarized band at 704 cm⁻¹. The Raman spectra of crystalline calcium magnesium orthosilicates do not show any band in this region (Piriou and McMillan, 1983a), while the band increases in intensity with increasing silica content (Virgo et al., 1980; Mysen et al., 1980a, 1982a; this work, Fig. 3). All of the above authors concluded that this 704 cm⁻¹ band was due to a symmetric stretching motion of or about the bridging oxygen in dimer units, Si₂O₇, within the glass structure. The presence of such units within a glass at the orthosilicate composition (sample 1; Table 1) suggests that some

oxygen within the glass is not bound to silicon, but only to magnesium and/or calcium.

With increasing silica content (samples 3 to 10), this band increases in intensity, becomes asymmetric, and shifts its maximum to lower frequency, to near 620 cm⁻¹ for sample 10 (Fig. 3). From studies of alkali silicate glass

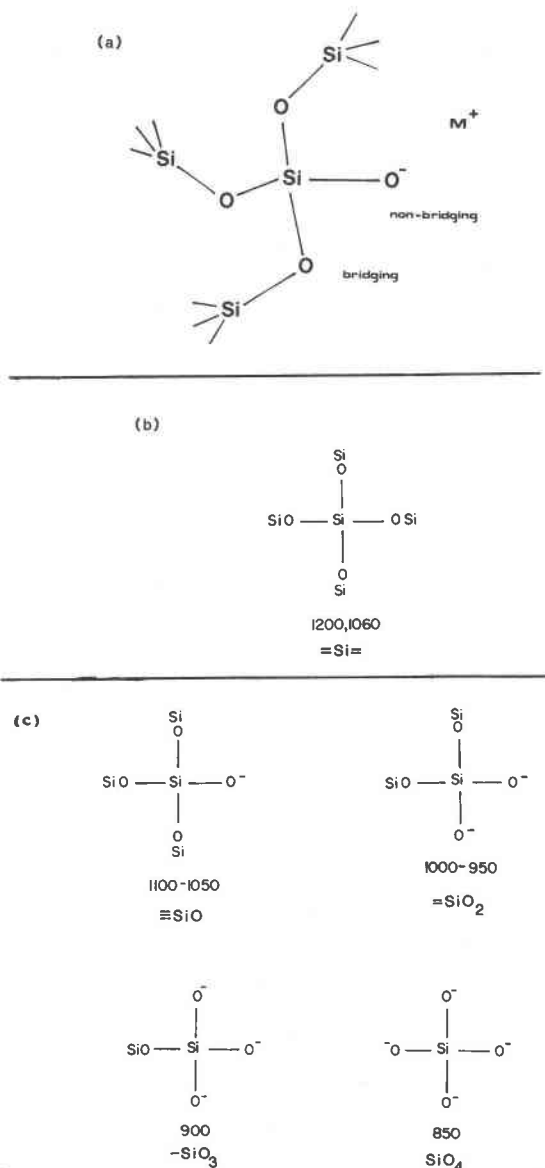


Fig. 6. Silicate structural units. (a) Schematic indicating the nature of bridging and non-bridging oxygen in the present context. M⁺ may also refer to 0.5 M²⁺, as in the alkaline earth series. (b) The weak, depolarized bands at 1200 and 1060 cm⁻¹ are assigned to asymmetric silicon-oxygen stretching vibrations within a fully-polymerized tetrahedral network =Si=. (c) The four major polarized high-frequency bands are generally assigned to symmetric stretching vibrations of tetrahedral silicate units with one, two, three and four non-bridging oxygens.

series (e.g., Brawer and White, 1975; Konijnendijk and Stevels, 1976; Verweij and Konijnendijk, 1976; Furukawa et al., 1981) it is likely that the dominant 430 cm^{-1} band of vitreous silica represents the continuation of this band to high silica content. The band is always highly polarized (Verweij, 1979a,b; this work, Fig. 3). The asymmetry of this band in these room-temperature spectra is partly due to thermal population effects, and may partly be due to the presence of discrete component bands as for the high-frequency band group. Attempts at curve-fitting using up to six Gaussian components were unsuccessful, and the problem was deemed too unconstrained for meaningful deconvolution at the present level.

All of the previous studies on this and similar systems (see McMillan, 1984) have associated the $400\text{--}700\text{ cm}^{-1}$ band with the presence of bridging oxygens corner-shared between adjacent SiO_4 tetrahedra (see Fig. 6), indicating silicate units more polymerized than the isolated orthosilicate tetrahedron. The detailed motions giving rise to this low-frequency band are as yet unclear, and may change as a function of the particular silicate group involved. Isotopic studies on Si_2O_7 dimers in crystalline pyrosilicates suggest considerable silicon motion associated with the 700 cm^{-1} vibration (Tarte et al., 1973), consistent with its assignment to a symmetric stretch of the $-\text{SiO}_3$ groups about their bridging oxygen (e.g., Lazarev, 1972, p. 63–72). However, the 430 cm^{-1} band of vitreous silica shows a large $^{18}\text{O}/^{16}\text{O}$ isotopic shift consistent with mainly oxygen motion, suggested to be in the plane bisecting the Si–O–Si bridge (e.g., Galeener and Mikkelsen, 1981).

The mid-range region. Vitreous silica shows an asymmetric band near 800 cm^{-1} , with probable components at 790 and 830 cm^{-1} (e.g., Seifert et al., 1982). Comparison of VV and VH spectra shows that the lower frequency component has a higher depolarization ratio (Fig. 3). Vibrational calculations have associated modes in this region with mainly motion of silicon (e.g., Laughlin and Joannopoulos, 1977; Furukawa et al., 1981), consistent with the results of the isotopic exchange studies of Galeener and Mikkelsen (1981) and Galeener and Geissberger (1983). Laughlin and Joannopoulos (1977) and Piriou and McMillan (1983b) suggested that the silicon motion was symmetric about the bridging oxygens, consistent with the observed infrared and Raman intensities (see McMillan et al., 1982). In alkali silicate glass systems, this band broadens and shifts to slightly lower frequency with decreasing silica content, to around 750 cm^{-1} at 55 mole % silica (e.g., Brawer and White, 1975; Verweij and Konijnendijk, 1976; Furukawa et al., 1981; Mysen et al., 1982a). The band is observed in the present $\text{SiO}_2\text{--CaMgSiO}_4$ glasses as a weak shoulder in the VV spectra, and as an asymmetric band near 780 cm^{-1} in the VH spectra (Fig. 3; also Virgo et al., 1980; Mysen et al., 1980a, 1982a). This band may not be clearly distinguished for samples with less than 50 mole % silica.

It is possible that the mid-range bands in these silicate glass series are similar to the 800 cm^{-1} band of vitreous

silica, and due predominantly to motion of silicon against its oxygen "cage". It is of interest that bands are observed in this region in the infrared and Raman spectra of crystalline sheet silicates (e.g., Brawer and White, 1975; Pavinich et al., 1976; Verweij and Konijnendijk, 1976; Verweij, 1979b), but not in the spectra of calcium magnesium chain silicates (e.g., Etchepare, 1970a, 1972; Omori, 1971; White, 1975; Zulumyan et al., 1976; Conjeaud and Boyer, 1980). McMillan (1981) suggested that such "silicon cage motions" might only be resolved in silicate structures with a high degree of polymerization where associated oxygen motion would be hindered, and that these vibrations might couple with vibrations of the bridging oxygens (giving rise to the $700\text{--}400\text{ cm}^{-1}$ band set) for lower silicate polymerizations.

The $\text{SiO}_2\text{--CaMgSiO}_4$ miscibility gap

Three samples were prepared with bulk compositions within the $\text{SiO}_2\text{--CaMgSiO}_4$ two-liquid field (Fig. 1). One set of glasses was prepared by normal quenching, and gave opaque samples which were macroscopically inhomogeneous and presumably unmixed (Table 1 and inset to Fig. 7). A second set were re-melted then super-quenched, to give optically transparent glasses which were much more homogeneous to electron microprobe analysis (Table 1). Sample 12 had a bluish tinge, but samples 11 and 13 were colorless, implying inhomogeneities smaller than several hundred Angstroms (Voishvillo, 1962; Andreev, 1978). The spectra of these two sets of glass samples are compared in Figure 7. Also shown are the spectra of vitreous silica and of sample 10, with compositions near the poles of the liquidus miscibility gap in the $\text{SiO}_2\text{--CaMgSiO}_4$ system (see Fig. 1).

The spectra of the normal-quenched opaque unmixed samples 11 to 13 are simple superpositions of the spectra of SiO_2 and sample 10, varying inversely in relative intensity as the two-liquid field is traversed. This is the expected behavior for a two-phase sample with varying relative proportions of each phase. It is of interest that the spectra of the super-quenched and optically transparent glasses show exactly the same behavior, which has several implications. First, the same vibrating units are present in both the opaque and the transparent samples, suggesting no difference in molecular structure between the two sets of samples as sampled by the Raman experiment. The major difference between the opaque and transparent samples then probably lies in the size of the individual structural units responsible for macroscopic inhomogeneity. Glass and liquid immiscibility is commonly detected and measured by the onset of visible opalescence in the sample (e.g., Haller et al., 1974) which occurs when density fluctuations are of the order of several hundred Angstrom units across (Voishvillo, 1962; Andreev, 1978). The present study shows that Raman spectroscopy is insensitive to size changes in the structural unit on a hundred Angstrom level, which would be consistent with Raman band localization arguments (see McMillan,

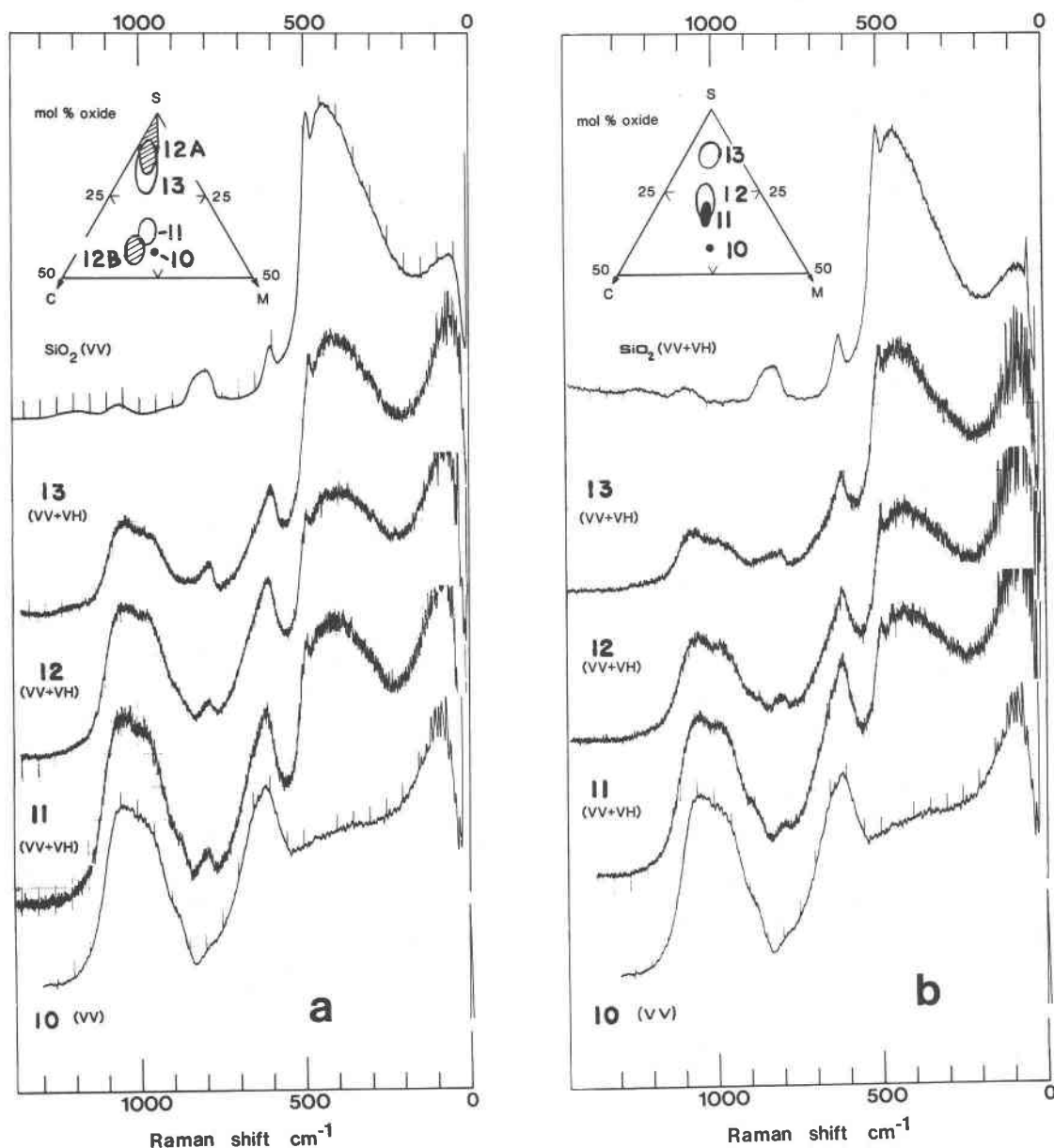


Fig. 7. Crossing the $\text{SiO}_2\text{-CaMgSiO}_4$ miscibility gap (samples 11, 12 and 13). Spectra (a) correspond to normal-quenched, opaque glasses, while (b) shows the spectra of super-quenched, transparent glasses of similar bulk compositions to those in (a). The samples in (b) were re-melted for super-quench, hence had slightly lower silica content due to volatilization (see text, and Table 1), which explains the band intensity differences between spectra (a) and (b).

1984). It also suggests that the molecular groups precursor to phase separation are present in the transparent glass series, which would classically be termed "homogeneous". This places limits on the structural significance of miscibility gaps determined by opalescence and clearing temperatures. Finally, there is no evidence in the $\text{SiO}_2\text{-CaMgSiO}_4$ glass series for intermediate structures between those at the poles of the classical miscibility gap, in contrast to the $\text{SiO}_2\text{-Na}_2\text{O}$ and $\text{SiO}_2\text{-K}_2\text{O}$ glass series

where a continuous set of changes is found (e.g., Etchepare, 1970b; Brawer and White, 1975; Konijnendijk and Stevels, 1976; Verweij and Konijnendijk, 1976; Furukawa et al., 1981; Mysen et al., 1982; Matson et al., 1983).

The $\text{SiO}_2\text{-CaO}$ and $\text{SiO}_2\text{-MgO}$ glass series

The unpolarized Raman spectra of glasses along the $\text{SiO}_2\text{-CaO}$ and $\text{SiO}_2\text{-MgO}$ joins are shown in Figure 8. The spectra are similar to those obtained in previous

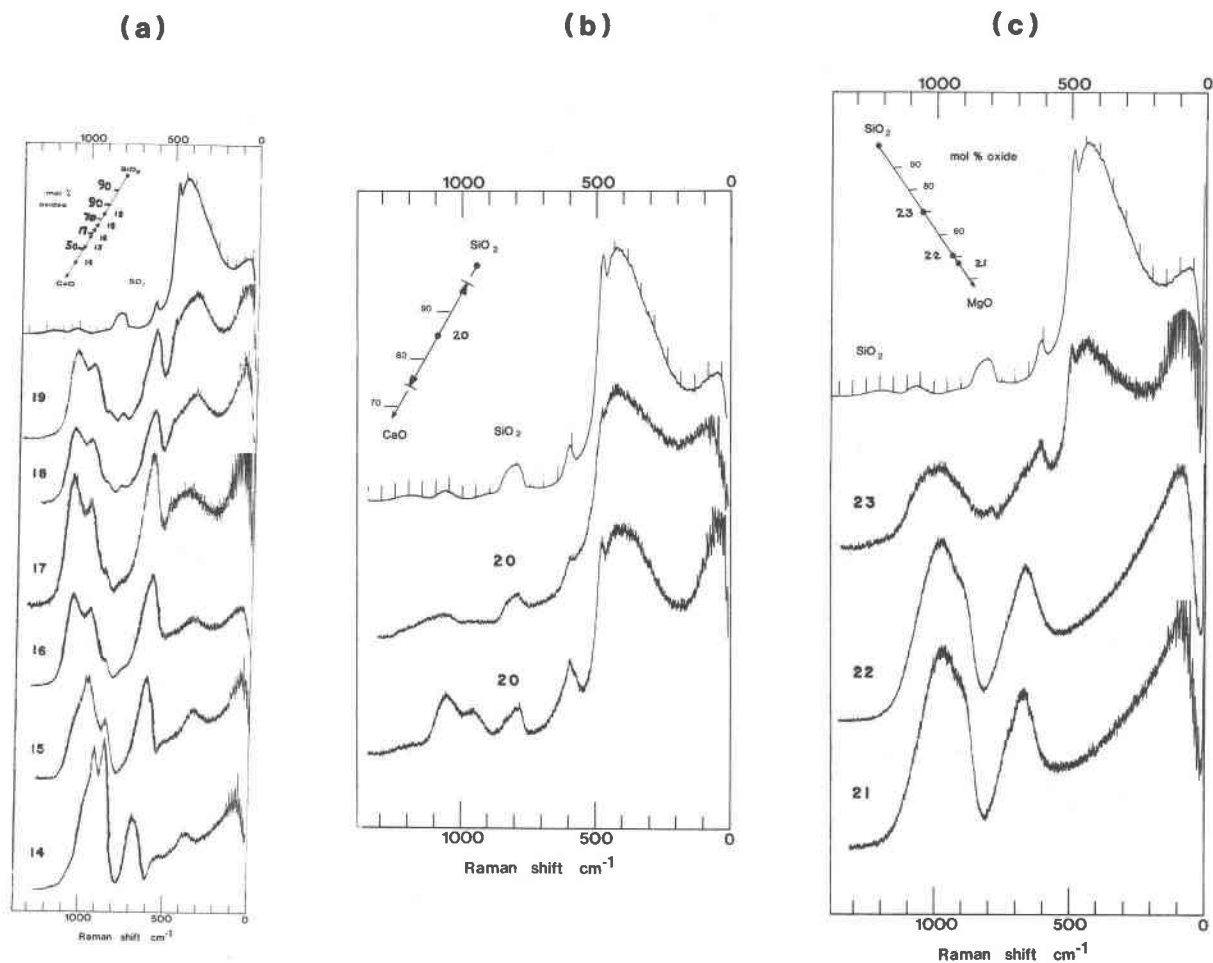


Fig. 8. Unpolarized (VV + VH) Raman spectra of glasses (a) 14–19 and (c) 21–23 and SiO_2 , respectively along the SiO_2 - CaO and SiO_2 - MgO joins. CaO-SiO_2 sample 20 (b) was opaque and inhomogeneous, with approximate compositional limits as shown in the inset. The two spectra were taken from different parts of the sample. From their form, these correspond to higher-silica and lower-silica regions.

studies (e.g., Kashio et al., 1980; Mysen and Virgo, 1980; Mysen et al., 1980a,b, 1982a,b; Tsunawaki et al., 1981) and show similar changes with silica content to the SiO_2 - CaMgSiO_4 glass series. The individual bands in the SiO_2 - CaO series are better-resolved than those for the SiO_2 - MgO glasses. Brawer and White (1977) studied series of sodium silicate glasses containing calcium or magnesium, and found the bands for the calcic glasses better-resolved than for the magnesian compositions. Some of the SiO_2 - CaO and SiO_2 - MgO samples had compositions within the CaO-MgO-SiO_2 two-liquid field, and both opaque unmixed and transparent "homogeneous" glasses were prepared by normal- and fast-quench techniques. As for the SiO_2 - CaMgSiO_4 series, both sets of samples had identical Raman spectra.

The binary calcium silicate sample 20 prepared by normal quenching was found to be very inhomogeneous, with a bulk composition near 85 mole % silica but

variations of ± 10 mole % in silica content within the sample (Table 1). A number of spectra were obtained from different parts of the sample, and none were exactly alike. The two most extreme spectra observed are shown in Figure 8b. The spectrum with higher intensity in the high-frequency region corresponds to the area with lower silica content. This low-silica spectrum is similar in form to the spectrum of samples 18 and 19, within the SiO_2 - CaO miscibility gap, but with different relative intensity of the high-frequency and low-frequency parts. These are generally indicative of the relative proportions of respectively low-silica and high-silica unmixed regions, as discussed above for the SiO_2 - CaMgSiO_4 series.

The spectrum for the higher silica part of sample 20 shows a different type of spectrum (Fig. 8b). The 430 cm^{-1} band of vitreous silica still dominates the spectrum, but its "defect" bands at 500 and 600 cm^{-1} seem suppressed relative to both SiO_2 glass and the lower-silica

part of sample 20. The high-frequency region shows only a weak, broad, asymmetric band, in contrast to the constant band pattern indicative of the depolymerized silicate units of the unmixed spectra. Polarization studies (not shown) indicate that this weak band is a combination of three bands. The depolarized bands of vitreous silica may be identified at 1060 and 1200 cm⁻¹, with a new polarized band appearing near 1100 cm⁻¹. This is similar to the spectra observed for silica glass with small additions of alkali oxides, M₂O (Stolen and Walrafen, 1976; Mysen et al., 1982; Matson et al., 1983), KAlO₂ (McMillan et al., 1982) and Al₂O₃ (McMillan and Piriou, 1982). It is suggested that the polarized 1100 cm⁻¹ band corresponds to the symmetric stretching vibration of a small proportion of ≡SiO units, within a silica glass framework only slightly perturbed by the presence of CaO component (see also McMillan and Piriou, 1982).

Interpretations and structural models

Consistent with the results of previous studies, the observed high-frequency bands have been assigned to silicon-oxygen stretching motions of =Si=, ≡SiO, =SiO₂, -SiO₃ and SiO₄ groups within the glass structure (see Fig. 6). Their observed relative intensity variation as a function of silica content is consistent with a decrease in the average polymerization of the silicate units as the silica content is decreased, and that some distribution of polymerized species is present at a given silica content (Figs. 3-5, 8; also e.g., Furukawa et al., 1981; Mysen et al., 1982a). Most previous studies have not considered the detailed arrangement of these molecular groups, only their relative distribution as a function of silica content (see McMillan, 1984). Brawer and White (1975) proposed that individual silicate tetrahedral units might show bond length and angle disorder, and that adjacent units could have different polymerization. This model allows for continuous depolymerization of the silica glass network on addition of metal oxide component, by creation of silicate tetrahedra with non-bridging oxygens at random throughout the structure. More recently Mysen, Virgo and co-workers (e.g., Virgo et al., 1980; Mysen et al., 1980a, 1982a) have proposed a model based on discrete anionic silicate structural units. At any given silica content, the melt or glass structure will contain a distribution of orthosilicate and pyrosilicate dimer groups, infinite chain and sheet structures, and three-dimensional network units. This latter model implies that the Raman bands used to characterize these long-range structures are in fact specific to such structures and exclude other possibilities, such as the random arrangement of silicate units proposed by Brawer and White (1975). A number of authors have discussed the localization of the dominant Raman bands in silicate glasses (e.g., Bell and Dean, 1970; Bell et al., 1970; Brawer, 1975; Furukawa et al., 1981; McMillan and Piriou, 1983; McMillan, 1984). It seems likely that the major high-frequency bands are highly localized within a given silicate tetrahedral unit,

and are relatively insensitive to the nature of adjacent tetrahedral units. This excludes the use of the high-frequency Raman bands of silicate glasses to characterize long-range structures such as infinite sheets and chains. This implies that although the Raman spectra are consistent with the model of Virgo et al. (1980) and Mysen et al. (1980a, 1982a), they are equally consistent with that of Brawer and White (1975). In the present article, the molecular groups ≡SiO, =SiO₂, and -SiO₃ are not assigned to any particular long-range structure. By definition, the groups SiO₄ and =Si= denote respectively a silicate tetrahedral unit with four non-bridging oxygens, and a silicate unit corner-sharing all four oxygens as part of a fully-polymerized network.

To investigate the effect of different metals on the distribution of silicate species, it is of interest to compare the spectra of glasses with the same silica content. This was done in the present study for CaO-MgO-SiO₂ glasses with near 70 mole % silica. The spectra of these glasses are shown in Figure 9. The high-frequency bands of the

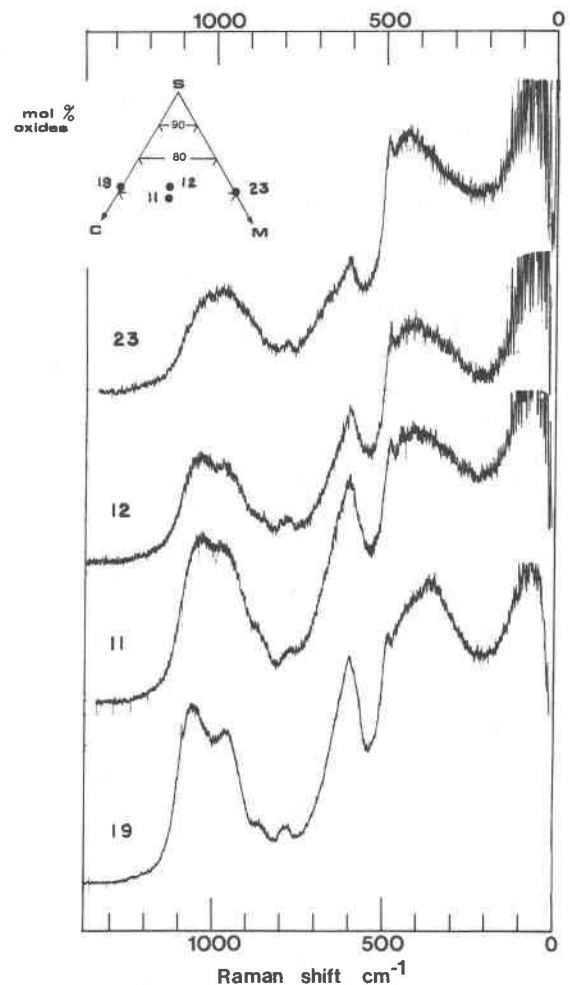


Fig. 9. The effect of calcium/magnesium substitution on the spectra of glasses with near 70 mole % silica.

CaO-SiO₂ glass (19) are well-resolved at 1060 and 970 cm⁻¹. The dominant 1060 cm⁻¹ band indicates a high proportion of ≡SiO units, while the 970 cm⁻¹ is due to =SiO₂ groups. The weak band at 860 cm⁻¹ indicates the presence of isolated SiO₄ tetrahedra. The 900 cm⁻¹ band expected for -SiO₃ groups is probably unresolved from the higher frequency group (see Figs. 3 and 4; also Mysen et al., 1982b). The SiO₂-CaMgSiO₄ samples 11 and 12 have silica contents of respectively 68 and 72 mole % silica. The high-frequency bands are less well-resolved than those of the calcic glass. The 1060 cm⁻¹ band remains more intense than the shoulder at 980 cm⁻¹; but less so than for sample 19. Finally, the SiO₂-MgO glass (23) shows no bands resolved at high frequency, but only a broad asymmetric maximum between 960 and 1080 cm⁻¹, where the lower-frequency part seems to predominate. These observations suggest that, if Mg/Ca substitution affects the absolute intensities of the 1060 and 970 cm⁻¹ bands in the same way, the relative proportion of =SiO₂ to ≡SiO groups increases as magnesium is substituted for calcium in the glass structure.

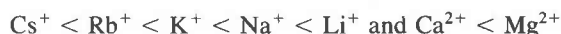
Related observations have been noted in studies of other silicate glass systems. The spectra of alkali silicate glasses with above 60 mole % silica are dominated by a band near 1100 cm⁻¹ due to ≡SiO units with a weaker band near 950 cm⁻¹ associated with =SiO₂ groups (e.g., Brawer and White, 1975; Verweij and Konijnendijk, 1976; Konijnendijk and Stevels, 1976). Brawer and White (1975) noted that the 950 cm⁻¹ band was relatively more prominent in the order K < Na < Li, at a given silica content. Matson et al. (1983) have obtained Raman spectra for a wider range of alkali silicate glasses, and find that the relative intensity of the 950 cm⁻¹ band increases in the sequence Cs < Rb < K < Na < Li at fixed silica content. This band was also observed to appear at higher silica content in these glass series in the same order. At the same time, there is an increased intensity near 450 cm⁻¹ in the same order, attributed to an increased proportion of silica-like network (=Si= units) in the glass structure. Brawer and White (1977) studied series of high-silica CaO-Na₂O-SiO₂ and MgO-Na₂O-SiO₂ glasses. They observed increased proportions of =SiO₂ and =Si= units relative to ≡SiO groups as the alkaline earth cation was substituted for sodium, with magnesium having more effect than calcium. Finally, the results of Mysen et al. (1982a) for SiO₂-Na₂O, BaO, CaO and (Ca,Mg)O glass series show that, at given high silica content, the 1000-950 cm⁻¹ band indicative of =SiO₂ units is relatively more important in the order Na < Ba < Ca (Ca,Mg), compared with the 1100-1050 cm⁻¹ band associated with ≡SiO units. These observations may be rationalized by the following model, termed the "molecular site model" (McMillan, 1981; McMillan and Piriou, 1983).

If it assumed that all oxygen is coordinated to silicon, and that local electrostatic charge balance must be satisfied, then a given metal cation will have an appropriate combination of bridging and non-bridging oxygens in its

coordination sphere. The non-bridging oxygens may be described by the silicate molecular units SiO₄, -SiO₃, =SiO₂ and ≡SiO, and may be used to define types of cation site. The model is most simply discussed for high silica content, where =SiO₂, ≡SiO and uncharged =Si= units predominate, and for singly- and doubly-charged cations M⁺ and M²⁺. A single site ≡SiO defines a site for one M⁺ cation, while the doubly-charged site =SiO₂ may accommodate one M²⁺, or two M⁺ cations. Finally, a coupled site [≡SiO]₂, with two discrete ≡SiO units within the coordination sphere, may be formulated to house a single M²⁺ or two M⁺ cations. The uncharged unit =Si= has no associated cation. At a given silica content, the relative proportion of these sites will be a function of the metal cation. Large cations M⁺ should prefer the single site ≡SiO, since occupation of =SiO₂ sites would lead to steric crowding, while smaller M⁺ cations should allow a higher proportion of =SiO₂ sites. Doubly-charged cations M²⁺ of large ionic radius should preferentially occupy the more open, coupled site [≡SiO]₂, while smaller M²⁺ cations will favor the higher charge concentration offered by the =SiO₂ sites. At constant silica content, the overall distribution of silicate molecular units is fixed by the "reaction"



The above reasoning suggests that this reaction will be driven to the right for small, doubly-charged cations, and to the left for large, singly-charged cations. This is consistent with the experimental observations discussed above, where bands for =SiO₂ and =Si= units become more prominent at the expense of ≡SiO groups, at similar silica content in the order



The formation of =Si= and =SiO₂ units from ≡SiO groups is a charge concentration effect, since the =Si= unit has no associated cation. The clustering induced by this charge concentration may be regarded as incipient immiscibility, and suggests that the tendency for unmixing should increase in the order Cs < Rb < K < Na < Li for the alkalis, and Ca < Mg for the alkaline earth silicates. The model also suggests that the low-silica limit of the two-phase region should move toward more basic compositions, in the same order.

It has long been known that liquids in the systems SiO₂-MgO, CaO and SrO show large miscibility gaps at high silica content (e.g., Greig, 1927), while SiO₂-BaO and SiO₂-Li₂O, Na₂O and perhaps K₂O show metastable immiscibility in high silica glasses (e.g., Charles, 1966, 1967, 1969; Galakhov and Varshal, 1973; Haller et al., 1974; Hess, 1977). In all cases, the silica-rich liquid is near pure silica (90-100 mole % SiO₂), while the composition of the metal oxide-rich liquid or glass becomes progressively richer in metal oxide in the order Ba < Sr < Ca < Mg for alkaline earth oxides, and for the alkalis, K < Na < Li, with Li between Mg and Ca, Na between Sr

and Ba, and K lower than Ba (e.g., Kracek, 1939; Charles, 1967; Galakhov and Varshal, 1973; Hess, 1977). The above model based on the Raman spectroscopic results is certainly consistent with the observed immiscibility behavior of alkali and alkaline earth silicate melts and glasses. Matson et al. (1983) have recently developed a similar but independent model from their Raman studies of alkali silicate glasses. The model has also been extended to simple aluminosilicate compositions by McMillan et al. (1982) and Navrotsky et al. (1982), where it successfully rationalized heats of mixing along the SiO₂–NaAlO₂ and SiO₂–Ca_{0.5}AlO₂ glass joins, and predicted some tendency for unmixing in the system SiO₂–Mg_{0.5}AlO₂.

In all of the alkali and alkaline earth silicate miscibility gaps described above, the high silica limit of the two-phase region lies near 90–95 mole % silica, suggesting that a few per cent metal oxide component may dissolve in the silica glass network before leading to macroscopic phase separation. The spectrum of the high-silica SiO₂–CaO glass 20 (Figure 8b) shows a weak band assigned to ≡SiO units near 1100 cm⁻¹ between the two silica bands at 1060 and 1200 cm⁻¹. The major features of the silica glass spectrum are not changed, except that the two defect peaks at 500 and 600 cm⁻¹ are less prominent than in vitreous silica. It is suggested that these few per cent of metal oxide component may be accepted into the silica glass structure with formation of some ≡SiO units, without disrupting the overall glass network, and that this mechanism may suppress the structural "defect" responsible for the 500 and 600 cm⁻¹ bands. A similar effect was noted for small additions of Al₂O₃ to silica glass (McMillan and Piriou, 1982), and also for additions of KAlO₂ and alkali oxides where no stable immiscibility is known (e.g., Stolen and Walrafen, 1976; McMillan et al., 1982; Mysen et al., 1982a; Matson et al., 1983).

The above site model appears to give a useful molecular description of structural factors possibly responsible for the unmixing behavior observed in simple silicate systems. The model becomes of less value as the silica content is decreased, with formation of –SiO₃ and SiO₄ groups. Associated with these would be various combinations of M⁺ and M²⁺ cations, each controlled by a variety of factors, such as cation–oxygen bonding, and cation–cation repulsion effects. The sites –SiO₃ and SiO₄ may also be considered coupled to =SiO₂ and ≡SiO, further complicating the problem. Similarly, the model may not yet be simply formulated for higher valence cations. Finally, it is noted that the model will work best when electrostatic charge balance is most rigorous, or when the cation–oxygen association is maximized. However, as this association is increased, it may perturb the silicate bonding interaction. It is of interest that the major silicate bands are observed to broaden in the order Cs < Rb < K < Na < Li < Ca < Mg in alkali and alkaline earth silicate glass systems, which may partly reflect an increased perturbation of the silicate units as the cation strength increases.

Acknowledgments

This work has been supported by NSF grants EAR-7809954, INT-7926523, INT-8006965 and EAR-8108748, the French CNRS and the PIRPSEV program. The author would like to thank Bernard Piriou, John Holloway and Alex Navrotsky for their support and encouragement, Paul Caro of C.N.R.S. Bellevue for his hospitality, and Jean Etchepare of ENSTA Palaiseau for the use of his instrument to obtain spectra for samples of poor optical quality. He also thanks John Bradley, Jim Clark and Ann Yates at Arizona State University, and the analytical group at l'Université de Paris VI, for assistance with sample analyses, Mary McMillan for help with computing and drafting, and Nita Dagon and Mike Palitz for typing. A predecessor of this manuscript was reviewed by Bjorn Mysen, and in its present form was read by John Clemens, Chris Capobianco, Nancy Ross and Mike O'Keeffe and reviewed by Ed Stolper and Shiv Sharma, whose helpful comments were all appreciated.

References

- Andreev, N. S. (1978) Scattering of visible light by glasses undergoing phase separation and homogenization. *Journal of Non-Crystalline Solids*, 30, 99–126.
- Bell, R. J. and Dean, P. (1970) Atomic vibrations in vitreous silica. *Discussions of the Faraday Society*, 50, 55–61.
- Bell, R. J., Dean, P. and Hibbins-Butler, D. C. (1970) Localization of normal modes in vitreous silica, germania and beryllium fluoride. *Journal of Physics C*, 3, 2111–2118.
- Boyd, F. R. and Finger, L. W. (1975) Homogeneity of minerals in mantle rocks from Lesotho. *Carnegie Institute of Washington Yearbook*, 74, 519–525.
- Brawer, S. A. and White, W. B. (1975) Raman spectroscopic investigation of silicate glasses. I. The binary alkali silicates. *Journal of Chemical Physics*, 63, 2421–2432.
- Brawer, S. A. (1975) Theory of the vibrational spectra of some network and molecular glasses. *Physical Review B*, 1, 3173–3194.
- Brawer, S. A. and White, W. B. (1975) Raman spectroscopic investigation of the structures of silicate glasses (II). Soda-alkaline earth-alumina ternary and quaternary glasses. *Journal of Non-Crystalline Solids*, 23, 261–278.
- Charles, R. J. (1966) Metastable liquid immiscibility in alkali metal oxide-silica systems. *Journal of the American Ceramic Society*, 49, 55–62.
- Charles, R. J. (1967) Activities in Li₂O-, Na₂O- and K₂O–SiO₂ solutions. *Journal of the American Ceramic Society*, 50, 631–641.
- Charles, R. J. (1969) The origin of immiscibility in silicate solutions. *Physics and Chemistry of Glasses*, 10, 169–178.
- Conjeaud, M. and Boyer, H. (1980) Some possibilities of Raman microprobe in cement chemistry. *Cement and Concrete Research*, 10, 61–70.
- Coutures, J. P., Berjoan, R., Benezech, G., and Granier, B. (1978) Utilisation des fours solaires de laboratoire pour l'étude à haute température des propriétés physicochimiques des oxydes réfractaires. *Revue Internationale des Hautes Températures et Réfractaires*, 15, 103–114.
- Englehardt, G., Zeigan, D., Jancke, H., Hoebbel, D., and Wieker, W. (1975) Zur abhängigkeit der struktur der silicatanionen in wässrigen natrium silicatlösungen vom Na:Si verhältnis. *Zeitschrift für Anorganische Allgemeine Chemie*, 418, 17–28.

- Etchepare, J. (1970a) Spectres Raman du diopside cristallisé et vitreux. *Comptes Rendus de l'Académie des Sciences à Paris*, série B, 270, 1339-1342.
- Etchepare, J. (1970b) Sur l'interprétation des spectres de diffusion Raman de la silice vitreuse et de verres binaires de silicates alcalins. *Journal de Chimie Physique*, 67, 890-894.
- Etchepare, J. (1972) Study by Raman spectroscopy of crystalline and glassy diopside. In R. W. Douglas and B. Ellis, Eds., *Amorphous Materials*, p. 337-346. John Wiley and Sons, New York.
- Furukawa, T. and White, W. B. (1980) Vibrational spectra and glass structure. *Journal of Non-Crystalline Solids*, 38/39, 87-92.
- Furukawa, T., Fox, K. E., and White, W. B. (1981) Raman spectroscopic investigation of the structure of silicate glasses. III. Raman intensities and structural units in sodium silicate glasses. *Journal of Chemical Physics*, 75, 3226-3237.
- Galakhov, F. Ya. and Varshal, B. G. (1973) Causes of phase separation in simple silicate systems. In *The Structure of Glass*, vol. 8, *Phase Separation Phenomena in Glasses*, ed. E. A. Porai-Koshits, p. 7-11. Consultants Bureau, New York.
- Galeener, F. L. and Mikkelsen, J. C. (1981) Vibrational dynamics in ^{18}O -substituted vitreous SiO_2 . *Physical Review B*, 17, 1928-1933.
- Galeener, F. L. and Geissberger, A. E. (1983) Vibrational dynamics in ^{30}Si -substituted vitreous SiO_2 . *Physical Review B*, 27, 6199-6204.
- Greig, J. W. (1927) Immiscibility in silicate melts. *American Journal of Science*, 13, 1-44 and 133-154.
- Haller, W., Blackburn, D. H., and Simmons, J. H. (1974) Miscibility gaps in alkali-silicate binaries—data and thermodynamic interpretation. *Journal of the American Ceramic Society*, 57, 120-126.
- Hass, M. (1969) Temperature dependence of the Raman spectrum of vitreous silica. *Solid State Communications*, 7, 1069-1071.
- Heinrich, K. F. J. (1972) A simple correction procedure for quantitative electron probe microanalysis. National Bureau of Standards Technical Note 719, U.S. Government Printing Offices.
- Herzberg, G. (1945) *Molecular Spectra and Molecular Structure Vol. II, Infrared and Raman spectra of Polyatomic Molecules*. Van Nostrand Press.
- Hess, P. C. (1977) Structure of silicate melts. *Canadian Mineralogist*, 15, 162-178.
- Kashio, S., Iguchi, Y., Goto, T., Nishina, Y., and Fuwa, T. (1980) Raman spectroscopy study on silicate slag. *Transactions of the Iron and Steel Institute of Japan*, 20, 251-253.
- Konijnendijk, W. L. (1975) *The Structure of Borosilicate Glasses*, Philips Research Reports Supplements No. 1, Centrex Publishing Company, Eindhoven, Netherlands.
- Konijnendijk, W. L. and Stevels, J. M. (1976) Raman scattering measurements of silicate glasses and compounds. *Journal of Non-Crystalline Solids*, 21, 447-453.
- Laughlin, R. B. and Joannopoulos, J. D. (1977) Phonons in amorphous silica. *Physical Review B*, 16, 2942-2952.
- Lazarev, A. N. (1972) *Vibrational Spectra and Structure of Silicates*. Consultants Bureau, New York.
- Leadbetter, A. J. and Stringfellow, M. W. (1974) The frequency spectrum of the normal modes of vibration of vitreous silica and α -quartz. In *Proceedings of the Grenoble Conference on Neutron Inelastic Scattering*, p. 501-513. International Atomic Energy Association, Vienna.
- Levin, E. M., Robbins, C. R., and McMurdie, H. F. (1964) *Phase Diagrams for Ceramists*, Vol. I. American Ceramic Society, Columbus, Ohio.
- Matson, D. W., Sharma, S. K., and Philpotts, J. A. (1983) The structure of high-silica alkali-silicate glasses—a Raman spectroscopic investigation. *Journal of Non-Crystalline Solids*, 58, 323-352.
- McMillan, P. F. (1981) *A Structural Study of Aluminosilicate Glasses by Raman Spectroscopy*. Ph.D. dissertation, Arizona State University.
- McMillan, P. F. (1984) Structural studies of silicate glasses and melts—applications and limitations of Raman spectroscopy. *American Mineralogist*, 69, 622-644.
- McMillan, P. F. and Piriou, B. (1982) The structures and vibrational spectra of crystals and glasses in the silica-alumina system. *Journal of Non-Crystalline Solids*, 53, 279-298.
- McMillan, P. F. and Piriou, B. (1983) Raman spectroscopic studies of silicate and related glass structure: a review. *Bulletin de Minéralogie*, 106, 57-75.
- McMillan, P. F., Coutures, J. P., and Piriou, B. (1981) Diffusion Raman d'un verre de monticellite. *Comptes Rendus de l'Académie des Sciences à Paris*, série II, 292, 195-198.
- McMillan, P. F., Piriou, B., and Navrotsky, A. (1982) A Raman spectroscopic study of glasses along the joins silica-calcium aluminate, silica-sodium aluminate, and silica-potassium aluminate. *Geochimica et Cosmochimica Acta*, 46, 2021-2037.
- Mysen, B. O. and Virgo, D. (1980) Solubility mechanisms of carbon dioxide in silicate melts: A Raman spectroscopic study. *American Mineralogist*, 65, 885-899.
- Mysen, B. O., Virgo, D., and Scarfe, C. M. (1980a) Relations between the anionic structure and viscosity of silicate melts—a Raman spectroscopic study. *American Mineralogist*, 65, 690-710.
- Mysen, B. O., Seifert, F., and Virgo, D. (1980b) Structure and redox equilibria of iron-bearing silicate melts. *American Mineralogist*, 65, 867-884.
- Mysen, B. O., Virgo, D., Harrison, W. J., and Scarfe, C. M. (1980c) Solubility mechanisms of H_2O in silicate melts at high pressures and temperatures: a Raman spectroscopic study. *American Mineralogist*, 65, 900-914.
- Mysen, B. O., Ryerson, F. J., and Virgo, D. (1980d) The influence of TiO_2 on the structure and derivative properties of silicate melts. *American Mineralogist*, 65, 1150-1165.
- Mysen, B. O., Ryerson, F. J., and Virgo, D. (1981a) The structural role of phosphorus in silicate melts. *American Mineralogist*, 66, 106-117.
- Mysen, B. O., Virgo, D., and Kushiro, I. (1981b) The structural role of aluminum in silicate melts—a Raman spectroscopic study at 1 atmosphere. *American Mineralogist*, 66, 678-701.
- Mysen, B. O., Virgo, D., and Seifert, F. A. (1982a) The structure of silicate melts: implications for chemical and physical properties of natural magma. *Reviews of Geophysics and Space Physics*, 20, 353-383.
- Mysen, B. O., Finger, L. W., Virgo, D., and Seifert, F. A. (1982b) Curve-fitting of Raman spectra of silicate glasses. *American Mineralogist*, 67, 686-695.
- Navrotsky, A., Peraudeau, G., McMillan, P., and Coutures, J. P. (1982) A thermochemical study of glasses and crystals along the joins silica-calcium aluminate and silica-sodium aluminate. *Geochimica et Cosmochimica Acta*, 46, 2039-2047.
- Omori, K. (1971) Analysis of the infrared absorption spectrum of diopside. *American Mineralogist*, 56, 1607-1616.
- Pavinich, V. F., Mirgorodskii, A. P., Kolesova, V. A., and

- Lazarev, A. N. (1976) Interpretation of the infrared spectra of a laminated $\text{Li}_2\text{Si}_2\text{O}_5$ crystal and its structural analog $\alpha\text{-Na}_2\text{Si}_2\text{O}_5$. *Optics and Spectroscopy*, 40, 466-468.
- Piriou, B. and Alain, P. (1979) Density of states and structural forms related to physical properties of amorphous solids. *High Temperatures-High Pressures*, 11, 407-414.
- Piriou, B. and McMillan, P. (1983a) The high-frequency vibrational spectra of vitreous and crystalline orthosilicates. *American Mineralogist*, 68, 426-443.
- Piriou, B. and McMillan, P. (1983b) Ordre et spectroscopie vibrationnelle de silicates. *Bulletin de Minéralogie*, 106, 23-32.
- Seifert, F., Mysen, B. O. and Virgo, D. (1982) Three-dimensional network structure of quenched melts (glass) in the systems $\text{SiO}_2\text{-NaAlO}_2$, $\text{SiO}_2\text{-CaAl}_2\text{O}_4$ and $\text{SiO}_2\text{-MgAl}_2\text{O}_4$. *American Mineralogist*, 67, 696-717.
- Sharma, S. K. and Yoder, H. S. (1979) Structural study of glasses of akermanite, diopside, and sodium melilite compositions by Raman spectroscopy. *Carnegie Institute of Washington Yearbook*, 78, 526-532.
- Sharma, S. K., Virgo, D., and Mysen, B. O. (1979) Raman study of the coordination of aluminum in jadeite melts as a function of pressure. *American Mineralogist*, 64, 779-787.
- Shuker, R. and Gammon, R. W. (1970) Raman-scattering selection-rule breaking and the density of states in amorphous materials. *Physical Review Letters*, 25, 222-225.
- Stolen, R. H. and Walrafen, G. E. (1976) Water and its relation to broken bond defects in fused silica. *Journal of Chemical Physics*, 64, 2623-2631.
- Tarte, P., Pottier, M. J. and Procés, A. M. (1973) Vibrational studies of silicates and germanates - V. I. R. and Raman spectra of pyrosilicates and pyrogermanates with a linear bridge. *Spectrochimica Acta*, 29A, 1017-1027.
- Thomas, I. L. and Haukka, M. T. (1978) XRF determination of trace and major elements using a single-fused disc. *Chemical Geology*, 21, 39-50.
- Tsunawaki, Y., Iwamoto, N., Hattori, T., and Mitsuishi, A. (1981) Analysis of CaO-SiO_2 and $\text{CaO-SiO}_2\text{-CaF}_2$ glasses by Raman spectroscopy. *Journal of Non-Crystalline Solids*, 44, 369-378.
- Verweij, H. (1979a) Raman study of the structure of alkaligeranosilicate glasses (I): sodium and potassium metagermanosilicate glasses. *Journal of Non-Crystalline Solids*, 33, 41-53.
- Verweij, H. (1979b) Raman study of the structure of alkaligeranosilicate glasses II. Lithium, sodium and potassium digermanosilicate glasses. *Journal of Non-Crystalline Solids*, 33, 55-69.
- Verweij, H. and Konijnendijk, W. L. (1976) Structural units in $\text{K}_2\text{O-PbO-SiO}_2$ glasses by Raman spectroscopy. *Journal of the American Ceramic Society*, 59, 517-521.
- Virgo, D., Mysen, B. O. and Kushiro, I. (1980) Anionic constitution of 1-atmosphere silicate melts: implications for the structure of igneous melts. *Science*, 208, 1371-1373.
- Voishvillo, N. A. (1962) Coherent scattering of light in glass. *Optics and Spectroscopy*, 12, 225-229.
- White, W. B. (1975) Structural interpretations of lunar and terrestrial minerals by Raman spectroscopy. In C. Karr, *Infrared and Raman spectroscopy of Lunar and Terrestrial Materials*, p. 325-358. Academic Press, New York.
- Zulumyan, N. O., Mirgorodskii, A. P., Pavinich, V. F., and Lazarev, A. N. (1976) Study of calculation of the vibrational spectrum of a crystal with complex polyatomic anions. Diopside $\text{CaMgSi}_2\text{O}_6$. *Optics and Spectroscopy*, 41, 622-627.

*Manuscript received, March 1, 1983;
accepted for publication, January 25, 1984.*